Journal of Materials Chemistry C

ROYAL SOCIETY OF CHEMISTRY

PAPER

View Article Online
View Journal | View Issue

Cite this: J. Mater. Chem. C, 2020, 8, 2280

N-Heterocyclic carbene-ended polymers as surface ligands of plasmonic metal nanoparticles†

Srinivas Thanneeru,‡[a] Kaitlynn M. Ayers,‡[a] Murali Anuganti,[a] Lei Zhang,[a] Challa V. Kumar,[a] Gaël Ung *[a] and Jie He *[ab]

Received 29th August 2019,
Accepted 7th January 2020

DOI: 10.1039/c9tc04776j

rsc.li/materials-c

A facile methodology to prepare N-heterocyclic carbene (NHC)-terminated polymers as surface ligands to functionalize gold nanoparticles (AuNPs) is reported. Our method highlights a mild, aerobic synthesis of NHC-functionalized polymers and a simple ligand exchange approach towards surface modification of AuNPs prepared in aqueous solution. Two methods, including end-group functionalization of halogen-ended polymers from a conventional atom transfer radical polymerization (ATRP) and post-polymerization functionalization of imidazole-containing polymers using imidazole-containing ATRP initiator, have been investigated to prepare imidazolium-ended polymers. Using a one-step, oxygen and moisture tolerant procedure, the polymer–NHC–Cu(I) species can be synthesized from imidazolium-ended polymers and readily bind to citrate-capped AuNPs likely through transmetalation, yielding robust polymer-stabilized AuNPs. Our synthetic method significantly simplifies the preparation and use of polymer–NHC ligands for surface functionalization of metal NPs. Our methodology is general and potentially applicable to any polymers prepared by ATRP to functionalize metal NPs *via* NHC–metal coordination; therefore, it will likely broaden the applications of polymer–NHC ligands for metal nanoparticles in the fields of catalysis and nanomedicine.

1. Introduction

Surface ligands play a key role in stabilizing nanoparticles (NPs) in solution to prevent coalescence. A variety of either organic or inorganic molecules/ions (*e.g.*, surfactants, polymers, proteins, nucleic acids and inorganic ions) bound to surface atoms of NPs *via* metal–ligand coordination can be used as surface ligands for NPs. Synthetic polymers as ligands of NPs can enrich surface functionality, biocompatibility and responsiveness,[1–8] which are key features for applications in nanomedicine,[9,10] catalysis[11,12] and photonic materials.[13,14] Addition of polymer ligands to NPs is often achieved through ligand exchange of small-molecule-capped NPs by either end-functionalized polymers ("grafting to" method),[15–22] or by molecular initiators used to grow polymers later ("grafting from" method).[23–25] Thiol-ended polymers are the most popular polymer ligands for metal NPs, in particular when using the "grafting to" approach, due to the binding strength of the metal–thiolate interaction and the immediate availability of thiol-ended polymers prepared from reversible addition–fragmentation chain-transfer polymerization. However, early experiments in self-assembly monolayers suggest that thiol ligands are unstable and they are readily oxidized by oxygen or peroxides.[26,27]

N-Heterocyclic carbenes (NHCs) have gained continuous attention as surface ligands of metal NPs.[28–39] Due to the strong σ-donation of the carbene, NHCs bind strongly to metals *via* metal–carbon interactions.[40–42] Notably, NHC-supported NPs are more stable than thiol-capped NPs under harsh oxidative conditions[43] and have been shown to modulate the surface electron density of metal NPs as well as their catalytic activity.[11,12,44–47] Although ligand exchange using free NHCs to modify metal NPs (such as Au,[28,48] Pd,[44,49] and Pt[38]) have been reported, profound synthetic challenges remain in the "grafting to" approach, especially for polymer–NHC ligands. Surface modification of metal NPs utilizing free NHCs typically requires anaerobic and anhydrous conditions since free NHCs are air and water sensitive. This largely limits the use of free NHCs particularly for metal NPs synthesized and dispersed in aqueous solution. On the other hand, one can prepare polymer–NHC modified gold NPs (AuNPs) using chemical reduction of polymeric NHC–Au precursors,[34] although pre-synthesized AuNPs with well-defined size cannot be used directly. Moreover, our group recently demonstrated the "grafting to" approach for polymer NHC ligands using imidazolium-terminated polymers,[50] similar to small molecular NHC ligands.[30,51]

[a] Department of Chemistry, University of Connecticut, Storrs, CT 06269, USA. E-mail: Gael.ung@uconn.edu, Jie.he@uconn.edu
[b] Polymer Program, Institute of Materials Science, University of Connecticut, Storrs, CT 06269, USA

† Electronic supplementary information (ESI) available: Synthetic details of polymers, polymer–NHC–Cu(I) and surface ligand exchange methods as well as the additional characterization of polymer–NHC capped AuNPs. See DOI: 10.1039/c9tc04776j

‡ These authors contributed equally.

As an alternative, we herein present another robust and facile methodology to prepare NHC-functionalized polymers as surface ligands to functionalize AuNPs. Our method utilizes mild, aerobic synthetic conditions to prepare NHC-functionalized polymers and perform surface modification of metal NPs using NHC-ended polymers in aqueous solution. This potentially removes the synthetic obstacles of polymer–NHC ligand chemistry and makes polymer–NHC ligands accessible without complex syntheses. The synthetic strategy involves the preparation of polymer–NHC–Cu(I) complexes by post-polymerization functionalization of polymers prepared *via* atom transfer radical polymerization (ATRP) with an imidazolium end group, followed by treatment with Cu(I). Four polymer–NHC–Cu(I) complexes were prepared, including, polystyrene (PS), poly(methyl methacrylate) (PMMA), poly(*n*-butyl acrylate) (P*n*BA), and poly(2-(2-methoxyethoxy)ethyl methacrylate) ($PMEO_2MA$). These polymer–NHC–Cu(I) complexes were likely transmetalated to AuNPs at the water/oil interface, yielding robust polymer-stabilized AuNPs. The merit of our polymer–NHC ligand synthesis and exchange protocol is its versatility, since it can be extended to any polymers prepared by ATRP to functionalize metal NPs *via* NHC–metal coordination.

2. Experimental

2.1 Materials

All chemicals were purchased from Aldrich unless otherwise noted. Methyl methacrylate (MMA, 99%) and styrene (St, 99%) were passed through a basic aluminum oxide column prior to use. *N*,*N*,*N*′,*N*″,*N*″-Pentamethyldiethylenetriamine (PMDETA, >99%), *tert*-butyl α-bromoisobutyrate (BBiB, ≥98%), 2-bromo-2-methylpropionyl bromide (BMPB, 98%), copper(I) bromide (CuBr, 99.999% trace metal basis), anisole (anhydrous, 99.7%), copper(I) chloride (CuCl, ≥90% ACS reagent), gold(III) chloride hydrate ($HAuCl_4$, ≥99.0%), sodium citrate tribasic dihydrate (≥99.0%), dodecanethiol (DDT), potassium carbonate (K_2CO_3), phosphoric acid (H_3PO_4, >85%), glyoxal (40% in water), ^{13}C-paraformaldehyde (99%), and 1,4-dioxane (99.8%) were used as received. Methylamine (35.4% in water) was purchased from Alfa Aesar and ammonium chloride (NH_4Cl, crystals) were purchased from Macron Chemical. Plain gold SPR Reichert slides were purchased from Reichert technology. Deionized water (Millipore Milli-Q grade) with a resistivity of 18.0 MΩ was used in all the experiments.

2.2 Synthesis of PS and end-group functionalization

Synthesis of PS_{65}–Br. PS–Br was synthesized *via* ATRP using BBiB as an ATRP initiator. Styrene (20 g, 192.3 mmol) and CuBr (461.5 mg, 3.2 mmol) were mixed with 2 mL of anisole in a 25 mL round bottom flask with a magnetic stirrer. The flask was degassed and purged with N_2 for 5 min. Then, PMDETA (554.5 mg, 3.2 mmol) was added to the above solution and purged with N_2 for 10 more min. Finally, BBiB (711.5 mg, 3.2 mmol) in 1 mL of anisole was added and the mixture was purged with N_2 for another 15 min. The reaction was carried out at 80 °C and run for 1 h. The polymerization was quenched by adding 10 mL of dichloromethane (DCM) to the flask and the mixture was passed through a neutral alumina column to remove the copper catalyst. The solution was then concentrated by rotary evaporation and the resulting solution was precipitated three times in methanol, and then dried under vacuum at 40 °C. The number of repeat units for styrene was calculated to be 65 based on end-group analysis using the peak at 4.4 ppm in the ^{1}H NMR from the methine end group directly attached to the bromine atom in PS–Br. The obtained polymer has a M_n of 11.9 kg mol^{-1} and M_w/M_n ($Đ$) of 1.13 according to size elution chromatography (SEC) measurements using PS standards. Another polymer with a higher block length of styrene (PS_{186}–Br) was also prepared using the similar procedure described above. The PS_{186}–Br was characterized by both ^{1}H NMR spectroscopy and SEC. The PS_{186}–Br has a M_n of 18.1 kg mol^{-1} and $Đ$ of 1.12 according to SEC measurement.

Synthesis of PS_{65}–imidazolium (PS_{65}–Im). PS_{65}–Br (8.0 g, 1.16 mmol) and *N*-methylimidazole (1.93 g, 23.5 mmol) were dissolved in 20 mL of dimethylformamide (DMF) in a 50 mL round bottom flask with a magnetic stirrer. The flask was then placed in a pre-heated oil bath at 80 °C and stirred overnight. The obtained polymer was precipitated from methanol and dried under vacuum at 40 °C. The PS_{65}–Im has a M_n of 11.5 kg mol^{-1} and $Đ$ of 1.18 as per SEC measurement. The PS_{186}–Im polymer was also prepared under identical conditions.

Synthesis of PS_{65}–NHC–Cu(I). Preparation of NHC functionalized PS polymers were achieved according to a reported method in literature.[52] A 50 mL round bottom flask was charged with PS_{65}–Im (6.2 g, 0.89 mmol) and 40 mL of acetone was added. Then CuCl (188 mg, 1.89 mmol) and K_2CO_3 (260 mg, 1.89 mmol) were added to the stirring solution. The reaction was refluxed at 80 °C overnight. The solution was cooled to room temperature and passed through a medium glass frit with a plug of silica to remove the excess CuCl and K_2CO_3. The obtained polymer solution was concentrated and then precipitated in methanol and dried under vacuum at 40 °C. The obtained polymer has a M_n of 11.8 kg mol^{-1} and $Đ$ of 1.13 as per SEC measurements. Using the same conditions PS_{186}–NHC–Cu(I) was prepared. The PS_{186}–NHC–Cu(I) has a M_n of 18.0 kg mol^{-1} and $Đ$ of 1.11.

Synthesis of ^{13}C-labelled PS_{65}–^{13}C–Im and PS_{65}–^{13}CNHC–Cu(I). See ESI† for details.

Synthesis of imidazole-containing ATRP initiator and (meth)acrylate polymers. See ESI† for details.

2.3 Synthesis of AuNPs and surface modification of AuNPs

Synthesis of AuNPs. AuNPs with a size of 12 ± 1.0 nm were synthesized according to a previously reported citrate reduction method.[21] $HAuCl_4$ (100 mg) was dissolved in 1 L of deionized water and heated to reflux with stirring. Then, 30 mL of sodium citrate (1 wt%) aqueous solution was quickly injected into the reaction. After refluxing for 30 min, AuNPs with a size of 12 ± 1.0 nm were obtained.

Surface modification of AuNPs. The surface modification of AuNPs was performed *via* an interfacial ligand exchange method. To 50 mL of 12 nm AuNPs (0.093 mg mL^{-1}) in water, 30 mg of PS_{65}–NHC–Cu(I) in 30 mL of toluene was added in one

addition under sonication. An emulsion formed and the solution was stirred overnight to ensure complete ligand exchange (indicated by a colorless water phase). The oil phase containing PS-modified AuNPs was collected and purified by centrifugation 4 times at 9000 rpm. Centrifugation also ensures the removal of free polymers not bound to AuNPs. The NPs were then re-dispersed in tetrahydrofuran (THF) or other organic solvents as described in the main text. Note that the amount of polymer–NHC ligands is in a large excess to ensure the surface modification using "grafting to" approach and around 1% of polymers were actually bound to AuNPs based on TGA analysis. Please note that, all free polymers were removed from the modified AuNPs by centrifugation.

2.4 Characterizations

SEC measurements were performed on a Waters SEC-1 (1515 HPLC pump and Waters 717Plus auto injector) equipped with a Varian 380-LC evaporative light scattering detector and three Jordi Gel fluorinated DVB columns (1–100 K, 2–10 K, and 1–500 Å). THF was used as an eluent at a flow rate of 1.25 mL min^{-1}, and PS standards were used for molecular weight and molecular weight distribution calibration. The data sets were processed using Empower SEC software (Waters, Inc.). ^{1}H NMR spectroscopy was recorded on a Bruker AVANCE 400 MHz spectrometer. ^{13}C NMR spectroscopy was recorded on a Bruker AVANCE 500 MHz equipped with a 5 mm BBFO SmartProbe. The heteronuclear multiple bond correlation (HMBC) experiments were conducted on Varian INOVA 600 MHz spectrometer equipped with a triple-resonance ^{1}H, ^{13}C, ^{15}N cryogenic probe. An HMBC coupling constant (J) between ^{1}H and ^{13}C was set to 12 Hz. Transmission electron microscopy (TEM) was carried out on a JEOL 2010 TEM with an accelerating voltage of 200 kV. UV-vis spectra were recorded on a Cary 60 UV-vis spectrophotometer. For grafting density, thermogravimetric analysis (TGA) was performed using TA Instruments Q-500. Each sample was first dried at 100 °C for 60 min to remove any residual solvent. The analysis was performed by heating the samples from 100 to 700 °C at a heating rate of 10 °C per min under N_2.

3. Results and discussion

We first envisioned synthesizing imidazolium-ended polymers using end group functionalization of halogen-ended polymers prepared *via* ATRP. A bromine-ended PS_{65}–Br (M_n = 11 900 g mol^{-1} and $Đ$ = 1.18, Fig. S1, ESI†) was synthesized using *tert*-butyl α-bromoisobutyrate as an ATRP initiator and the end bromide was substituted with *N*-methylimidazole (Fig. 1a). The conversion of the Br end group to imidazolium (PS_{65}–Br to PS_{65}–Im) was confirmed using ^{1}H NMR spectroscopy (Fig. 1b). New peaks (d at 10.9 ppm and b, c at 7.8 ppm) are assigned to the N–C*H*–N, and vinyl protons of the imidazolium, respectively. The conversion of the Br end groups was estimated to be ~25% by integrating peak d from the imidazolium against peak a, the protons on the aromatic ring of PS. PS_{65}–Im was then treated with CuCl in presence of K_2CO_3 using a procedure similar to the one developed by Cazin and co-workers.[52] The disappearance of peak d of PS_{65}–Im

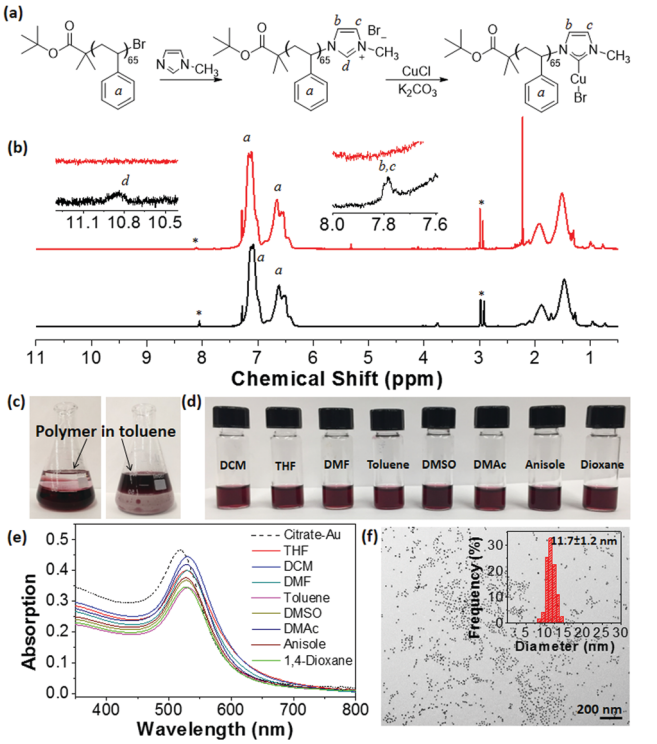

Fig. 1 (a) Synthesis of PS_{65}–NHC–Cu(I) using end group functionalization to convert Br to NHC–Cu(I). (b) ^{1}H NMR spectra of PS_{65}–Im (black, bottom) and PS_{65}–NHC–Cu(I) (red, top) measured in d-$CHCl_3$. *: residual DMF. (c) Images showing the transfer of citrate-capped AuNPs in water (bottom layer) to toluene (top layer) using PS_{65}–NHC–Cu(I). (d) Images showing the dispersion of PS_{65}–NHC modified AuNPs in various solvents. (e) UV-vis spectra showing the SPR absorption of AuNPs in various solvents. (f) TEM image of PS_{65}–NHC–Au in THF. The inset shows the average size of AuNPs.

(Fig. 1b) and shift of protons b and c indicates the formation of PS_{65}–NHC–Cu(I), as similar shifts are observed with a small molecule analogue (see Fig. S2, ESI†). We used Cu instead of Ag since Cu is more abundant and cheaper than Ag, while still being able to perform transmetalation in molecular complexes. In addition, Ag can form bis-carbene complexes with NHC. We ruled out the possibility of a bis-carbene $[(PS_{65}–NHC)_2Cu(I)]^+$ complex by studying the coordination chemistry of a small molecule analogue (Fig. S2 and Section S1 in ESI†).

The "grafting to" surface modification of citrate-capped AuNPs with PS_{65}–NHC–Cu(I) was performed using a biphasic ligand exchange method in a water/toluene mixture.[53,54] PS_{65}–NHC–Cu(I) was dissolved in toluene at a concentration of 1 mg mL^{-1} and added to an aqueous solution of citrate-capped AuNPs (0.093 mg mL^{-1}, ~12 nm in diameter, synthesized using a reported method[21]). After sonication, the mixture was stirred overnight. The phase transfer of AuNPs from water to toluene is evident from the deep red color in the toluene layer (Fig. 1c). After removal of the aqueous layer, AuNPs were collected by centrifugation and purified by five more centrifugations in chloroform. As a control, similar experiments were run using PS_{65}–Br and PS_{65}–Im in toluene. Phase transfer of AuNPs was not observed in these cases, indicating that the NHC–Cu(I) moiety is essential for surface modification (Fig. S3, ESI†).

PS-modified AuNPs were dispersed in several organic solvents to confirm the surface modification of AuNPs with PS_{65}–NHC. As shown in Fig. 1d, PS_{65}–NHC–Au is readily re-dispersed in any good solvent for PS, such as DCM, THF, DMF, toluene, dimethyl sulfoxide (DMSO), dimethylacetamide (DMAc), anisole and 1,4-dioxane. The corresponding UV-vis absorption spectra of PS_{65}–NHC–Au in various solvents clearly show the surface plasmon resonance (SPR) peak at 525–530 nm (Fig. 1e), indicative of excellent dispersity of AuNPs after ligand exchange. A slight red-shift of the SPR peak compared to the original citrate-capped AuNPs (518 nm) is attributed to the presence of polymers on the surface and differences in the refractive indexes of the solvents compared to water. The TEM image in Fig. 1f shows that PS_{65}–NHC–Au casted from THF is well-dispersed. The size of AuNPs measured from the TEM image is 11.7 ± 1.2 nm, comparable with that of citrate-capped AuNPs. Those results confirm the successful replacement of citrate ligands on the AuNPs by PS_{65}–NHC.

The change in surface hydrophobicity of PS_{65}–NHC–Au was investigated using water titration. When adding water to a THF solution of PS_{65}–NHC–Au, the solvent quality changes from good to poor for PS, resulting in the collapse of PS and the aggregation of AuNPs. The UV-vis spectra in Fig. 2a shows a clear red-shift in the SPR absorption peak from 528 nm to 565 nm when the concentration of water reached 38 vol%. The critical water concentration (CWC $\sim$20%) was estimated by the onset position of a sudden increase in the SPR peak when plotting the SPR peak absorption as a function of water concentration (Fig. 2b). This CWC value is close to that observed in AuNPs capped with thiol-ended PS, further confirming the presence of PS as surface ligands.[13] The red shift in SPR absorption reveals the formation of larger aggregates of AuNPs as confirmed by TEM (Fig. 2c). The stability of PS_{65}–NHC–Au towards the competing binding with 1-dodecanethiol was also investigated. It is stable to 10 mM of 1-dodecanethiol for 24 h, comparable to other NHC–AuNPs (Fig. S4, ESI†).[48,55]

A ^{13}C-labeled analogue, PS_{65}–^{13}CNHC–Cu(I), was used to examine the surface binding of polymer to AuNPs. The isotopically enriched imidazole N–^{13}CH–N was used to prepare PS_{65}–^{13}CIm (Fig. 3). The synthetic details and characterization of ^{13}C-labeled 1-methylimidazole are given in the ESI† (Section S3). The labeling and identity of PS_{65}–^{13}CIm was confirmed through both the chemical shift of N–^{13}CH–N in PS_{65}–^{13}CIm at 135 ppm in the ^{13}C NMR spectrum (Fig. 3c), and the proton peak of N–^{13}C*H*–N in PS_{65}–^{13}CIm appearing as a doublet at *ca.* 9.9–10.4 ppm in the ^{1}H NMR spectrum (Fig. S5, ESI†). Synthesis of the labeled carbene–Cu(I) complex (PS_{65}–^{13}CNHC–Cu(I)) was also confirmed by NMR spectroscopy. In the ^{13}C NMR spectrum, the N–^{13}C–N resonance shifted to 177 ppm (Fig. 3c). In the ^{1}H NMR spectrum, the diagnostic doublet for the proton peak of N–^{13}C*H*–N was no longer seen. The shifts and coupling in both ^{1}H and ^{13}C NMR spectra are consistent with changes observed in the small molecules and non-labeled polymers.

After modification of AuNPs with PS_{65}–^{13}CNHC–Cu(I), the ^{13}C NMR spectrum of PS_{65}–^{13}CNHC–Au did not show a clear peak for the N–^{13}CAu–N resonance, due to the relatively low grafting amount of polymers on the surface of the NPs and the immobilization that causes inefficient relaxation of the carbene carbon. A higher concentration was also difficult to obtain because of the scarcity of labeled materials, arising from the high cost of the labeled precursor. Therefore, a two dimensional ^{1}H–^{13}C HMBC experiment was performed to detect the N–^{13}CAu–N through its coupling to ^{1}H. Several protons could potentially correlate with N–^{13}CAu–N, including N–CH_3 and N–C*H*–CH_2 substituents of the imidazole. The experiment was calibrated for a J coupling of 12 Hz, in the range of typical imidazole $^{3}J_{H-C}$ (8–12 Hz).[56,57] Two strong cross peaks were observed as displayed in Fig. 3e. The first one is between a proton at 3.67 ppm (H_A) and a carbon at 171 ppm, which is assigned to the coupling of N–CH_3 with N–^{13}CAu–N. The chemical shift of N–CH_3 is closed to that shown in our model compound (Fig. S2, ESI†). The second cross peak is observed between a proton signal at 2.01 ppm (H_B) and the same carbon at 171 ppm, attributed to the coupling of benzyl protons of PS with N–^{13}CAu–N. The chemical shift suggests that, there is likely virtual coupling along the main chain of PS, since the chemical shift of the N–C*H*–CH_2 should appear at 5–6 ppm (Fig. S2, ESI†).

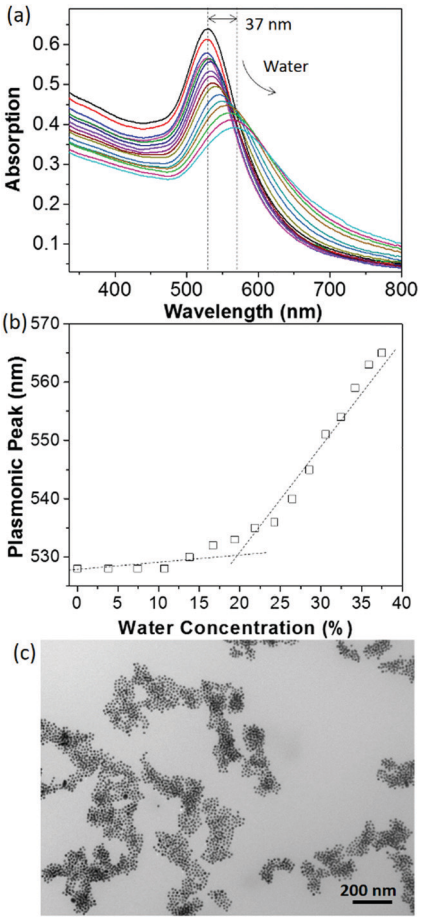

Fig. 2 (a) UV-vis spectra of PS_{65}–NHC modified AuNPs in THF when titrating with water. The spectra were collected by adding 80 μL of water each time into 2 mL of the THF solution of AuNPs. (b) Plotting the plasmonic peak of PS_{65}–NHC modified AuNPs as a function of water concentration to determine the critical water concentration. (c) TEM image of PS_{65}–NHC modified AuNPs in THF/water (1 : 1 vol) mixture.

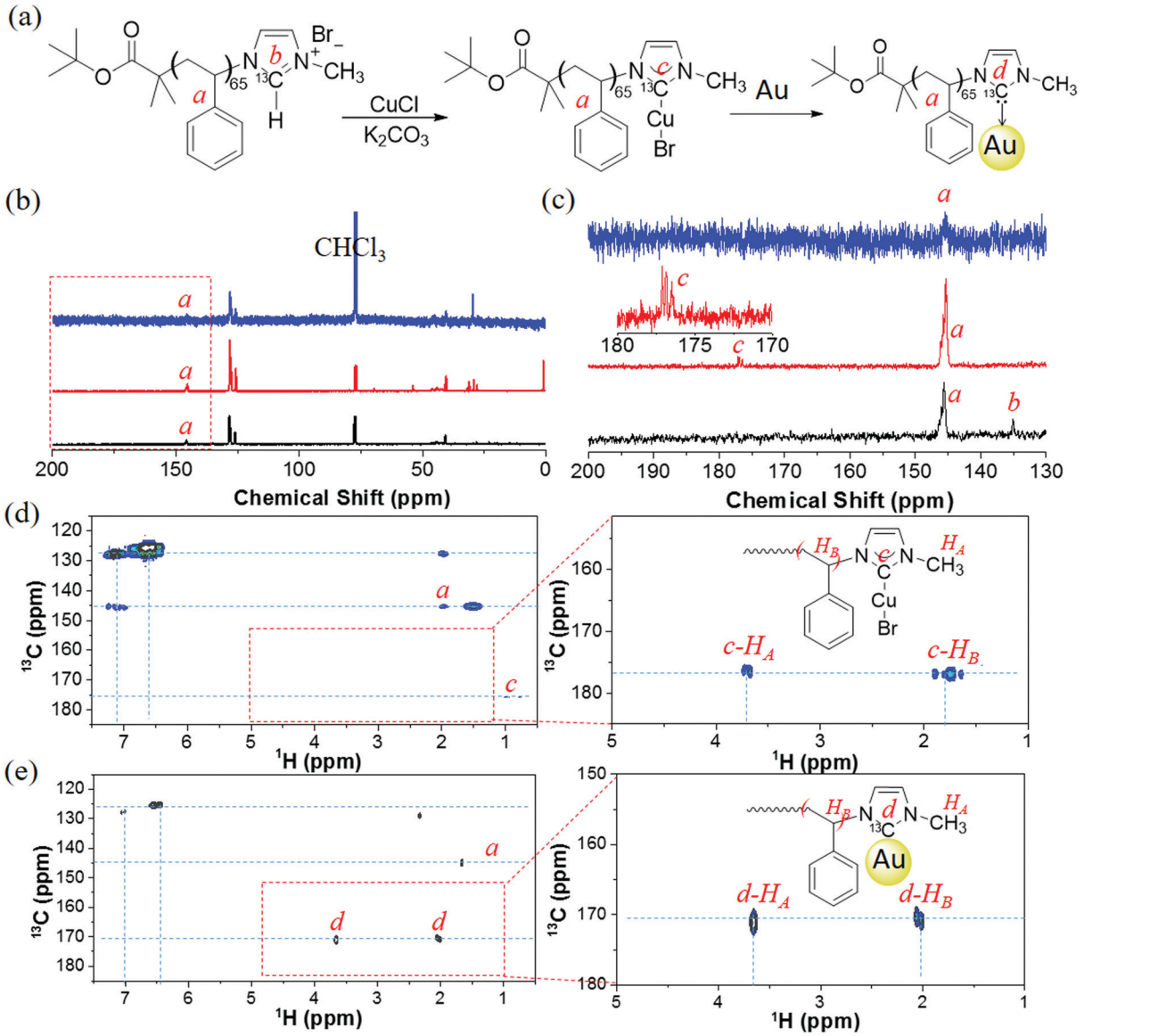

Fig. 3 (a) Synthesis of ^{13}C-labeled PS_{65}–^{13}C–NHC–Au using ^{13}C–Im. (b and c) ^{13}C NMR spectra of PS_{65}–^{13}C–Im (black, bottom), PS_{65}–^{13}C–NHC–Cu(I) (red, middle) and PS_{65}–^{13}C–NHC–Au (blue, top) in $CDCl_3$. ^{13}C NMR spectra in (b) in the range of 130–200 ppm is zoomed in (c). (d) 2D HMBC spectrum of non-labeled PS_{65}–NHC–Cu(I). (e) 2D HMBC spectrum of ^{13}C-labeled PS_{65}–^{13}CNHC–Au.

The new carbon resonance at 171 ppm is different than the signal of the N–^{13}*C*Cu–N precursor (177 ppm, Fig. 3b). To validate the observation of the ^{13}C signal through its coupling to H_A, we also ran the HMBC experiment with PS_{65}–NHC–Cu(I). Cross peaks between the N–^{13}*C*Cu–N carbon signal at 177 ppm and protons at 3.65 ppm (H_A, N–CH_3), 1.6–1.95 ppm and 0.9 ppm (main chain of PS) were observed (Fig. 3d). The resonance peak was identical with that from PS_{65}–^{13}*C*NHC–Cu(I) in Fig. 3c (the peak c in red line). We note that, the coupling of N–C*H*–CH_2 with N–^{13}*C*Au–N is weaker compared to that with free polymers PS_{65}–NHC–Cu(I) (refers to polymers before bound to AuNPs). This is presumably due to virtual coupling in free PS_{65}–NHC–Cu(I) (referred to non-immobilized polymers). Moreover, the chemical shift of N–^{13}*C*Au–N of PS_{65}–^{13}*C*NHC–Au is in the range of monometallic NHC–Au complexes,[58,59] NHC–AuNPs,[60,61] and NHC–Au clusters.[60,62] The upfield shift has also been reported previously when transferring NHC–Cu(I) to NHC–Au(I).[52,63] Therefore, the transmetalation from NHC–Cu(I) to Au(I) on the surface of AuNPs is likely the mechanism of our "grafting to" approach. However, on the other hand, the formation of metal–metal (Cu–Au) could be possible as well from a recent study using scanning tunneling microscope.[64] We do not outline this mechanism in the scheme of Fig. 3 to distinguish the surface modification on AuNPs from free PS_{65}–NHC–Cu(I). Regardless of NHC–Cu–Au or NHC–Au, PS_{65}–NHC–Cu(I) can readily modify AuNPs. We also note that the chemical shift of N–^{13}*C*Au–N in our results is much lower than those reported values from NHC–Au(0).[51,65,66] It is possible that polymers only form adsorbed molecular species on AuNPs, other than strongly bounded species.

The grafting density of PS_{65}–NHC ligands was evaluated by TGA (Fig. S6, ESI†). The density of PS_{65}–NHC ligands was estimated to be 0.33 chains nm^{-2}, corresponding to ~144 PS chains per AuNP. Compared to our results with thiol polymers that have similar molecular weight (1–4 polymer chains per nm^2),[16] the grafting density of PS_{65}–NHC ligands is low, likely due to the steric hindrance of the carbene. Nevertheless, another polymer possessing a longer block length, PS_{186}–NHC–Cu(I), was successfully utilized for the surface modification of AuNPs using the same methodology (Fig. S7, ESI†). These results demonstrate that our method can be generalized to transform halogen end groups to NHC–Cu(I) for polymers prepared *via* ATRP and use the NHC–Cu(I) end groups to functionalize metal NPs through a facile "grafting to" approach.

Although successful, our initial methodology is restricted by the low conversion of the bromine substitution by *N*-methylimidazole. We sought an alternative synthesis that incorporates the imidazole moiety as an end group. Instead of end-group post-polymerization, the imidazole end group can be included from an imidazole-containing ATRP initiator, 2-(1*H*-imidazol-1-yl)ethyl-2-bromo-2-methylpropanoate. Using this ATRP initiator, three imidazole-ended (meth)acrylate polymers were synthesized (see ESI† and Fig. S8 for details), including $PMMA_{85}$–Im (M_n = 7700 g mol^{-1} and $Đ$ = 1.16), P*n*BA_{104}–Im (M_n = 19 900 g mol^{-1} and $Đ$ = 1.09) and $PMEO_2MA_{125}$–Im (M_n = 20 000 g mol^{-1} and $Đ$ = 1.12) (see Fig. S9–S12, ESI†). Methylation using iodomethane followed by the metalation procedure presented above yielded all three corresponding NHC–Cu(I)-ended polymers. The incorporation of NHC–Cu(I) is much more efficient (close to 100%), compared to the substitution of end Br groups described above. Using $PMMA_{85}$–Im as an example, Fig. 4b shows the ^{1}H NMR spectra of $PMMA_{85}$–Im and metalated $PMMA_{85}$–NHC–Cu(I). The disappearance of peak f at 10.4 ppm, along with the shift of signals d and e confirms the coordination to Cu(I).

Surface modification of AuNPs with $PMMA_{85}$–NHC–Cu(I) was performed using a similar ligand exchange method at the interface of DCM and water. Because of the absence of aromatic groups in the polymer, this surface modification can be investigated by ^{1}H NMR spectroscopy. The two vinyl protons N–C*H*=C*H*–N from the imidazole ring of $PMMA_{85}$–NHC–Cu(I) have a chemical shift of 6.95 ppm (Fig. 4b).[28,67,68] After bound with AuNPs, the resonance of the two protons downshift to 6.87 ppm. The shift of the two vinyl protons towards values close to those reported for AuNPs[28,68] also confirms the surface binding with AuNPs. $PMMA_{85}$–NHC modified AuNPs show good dispersity in good solvents for PMMA such as THF, DMF, DMSO, DMAc, DCM, toluene, anisole and 1,4-dioxane (Fig. 4c). The UV-vis spectra of $PMMA_{85}$–NHC–Au dispersed in various solvents shows that the SPR absorption of our modified AuNPs is similar to that of citrate-capped AuNPs in water, indicating that there is no aggregation after dispersion in organic solvents (Fig. 4d). Likewise, stable and dispersed P*n*BA_{104}–NHC–Au was obtained utilizing the same methodology (Fig. S12, ESI†). It is worth noting that no successful examples have been reported using thiol-ended (meth)acrylate polymers solely to modify metal NPs through the "grafting to" method.

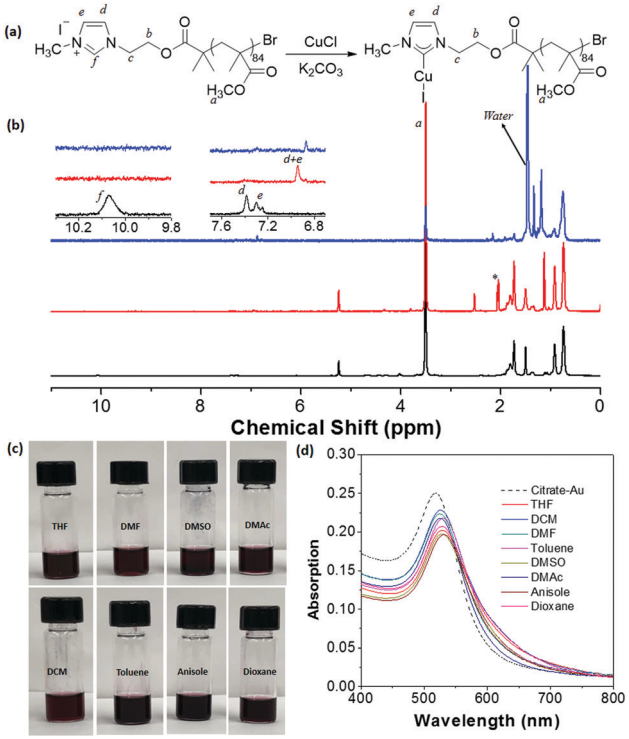

Fig. 4 (a) Synthesis of $PMMA_{85}$–NHC–Cu(I) using an imidazole-containing ATRP initiator. (b) ^{1}H NMR spectra of $PMMA_{85}$–Im (black, bottom), $PMMA_{85}$–NHC–Cu(I) (red, middle) and $PMMA_{85}$–NHC–Au (blue, top) in CD_2Cl_2. (c) Images showing $PMMA_{85}$–NHC–Au dispersed in various organic solvents. (d) UV-vis spectra showing the SPR absorption of $PMMA_{85}$–NHC–Au in various solvents.

To demonstrate the versatility of our method, hydrophilic $PMEO_2MA_{125}$–NHC–Cu(I) was also investigated to modify AuNPs (Fig. 5 and Fig. S13, ESI†). The $PMEO_2MA_{125}$–NHC–Au can be dispersed in a wide variety of organic solvents and water (Fig. 5b),

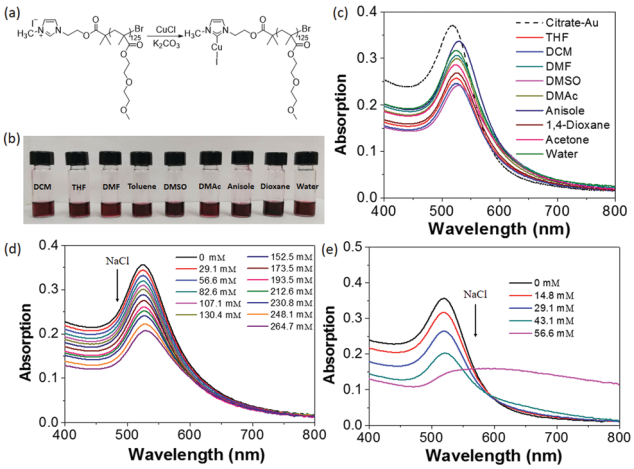

Fig. 5 (a) Synthesis of $PMEO_2MA_{125}$–NHC–Cu(I) using an imidazole-containing ATRP initiator. (b) Image showing solutions of $PMEO_2MA_{125}$–NHC–Au in various organic solvents and water. (c) UV-vis spectra showing the SPR peaks of AuNPs dispersed in various solvents. (d and e) Titration experiments showing the stability of $PMEO_2MA_{125}$–NHC–Au (d) and citrate-capped AuNPs (e) upon addition of 1 M NaCl.

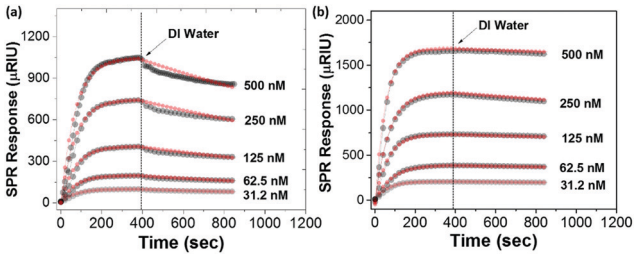

Fig. 6 SPR traces showing the binding kinetics of (a) $PMEO_2MA_{125}$–NHC–Cu(I) and (b) $PMEO_2MA_{174}$–SH to Au. After the flow of polymer solution, the DI water was flowed over the Au sensor to trace the dissociation. The thin red lines are the fit curves of the kinetic data.

suggesting that polymer ligands control the surface hydrophilicity of AuNPs. $PMEO_2MA_{125}$ modified AuNPs are stable in water and their aqueous solution can be stored for months without aggregation. The aqueous stability of $PMEO_2MA_{125}$–NHC–Au was examined against electrolyte-induced aggregation. While citrate-capped AuNPs aggregate when the NaCl concentration reached ~45 mM, $PMEO_2MA_{125}$–NHC–Au showed no sign of aggregation even at 265 mM NaCl (Fig. 5d and e), further confirming the stabilizing power of long-hydrophilic polymer ligands.

The binding strength of $PMEO_2MA_{125}$–NHC with the Au surface was estimated using SPR spectroscopy. $PMEO_2MA_{125}$–NHC–Cu(I) aqueous solutions at different concentrations were flowed over a plain Au surface sensor chip while monitoring the change of the SPR signal to follow the adsorption. Note that, it is a flat Au surface instead of the curved surface of AuNPs. After the adsorption reached equilibrium, the surface of the Au chip was washed with DI water and the dissociation of ligands was recorded (see details in Section S4 in ESI†). The SPR response of the adsorption of the $PMEO_2MA_{174}$–SH is approximately two times the response of $PMEO_2MA_{125}$–NHC–Cu(I) at the same concentration (Fig. 6), indicating a higher grafting density for the thiolated polymer to Au. The apparent binding constants are (K_a) is 7.7×10^7 M^{-1} and 7.1×10^8 M^{-1} for $PMEO_2MA$–NHC–Cu(I) and $PMEO_2MA_{174}$–SH, respectively (Table S2, ESI†). Although both values represent strong binding, the high grafting density of thiol groups on the surface of the Au chip will reduce the polymer chain dynamics, which in turn leads to a lower off-rate constant.

4. Conclusion

To summarize, we demonstrated a simple yet powerful methodology to prepare polymer–NHCs as surface ligands to functionalize AuNPs through a "grafting to" approach. Our method highlights the use of NHC–Cu(I) terminated polymers to modify AuNPs prepared in aqueous solution. Two approaches were outlined to directly convert polymers prepared from ATRP to imidazolium-ended polymers. In the first approach, the halogen end group on conventional polymers prepared through ATRP could be functionalized using *N*-methylimidazole to generate the imidazolium end group; while for the second approach, the imidazole end groups of polymers were converted to imidazolium through quaternization with CH_3I. Four polymers with NHC–Cu(I) end groups were obtained and readily bound to AuNPs through a biphasic ligand exchange method. The bonding from polymer–NHC–Cu(I) to polymer–NHC–Au was spectroscopically confirmed using HMBC with ^{13}C labeling on polymer–NHCs, likely through transmetalation. Syntheses of all materials from the initial end-group functionalization to the polymer–NHC supported AuNPs were carried out on the bench without any precautions taken to exclude air or moisture. Our methods can therefore be applied to virtually any polymers prepared from ATRP, which will greatly extend the scope of polymer–NHC ligand chemistry and enrich the library of polymer ligands to metal NPs.

Conflicts of interest

There are no conflicts to declare.

Acknowledgements

This work is supported by the startup fund of the University of Connecticut and ACS Petroleum Research Fund. The authors thank NMR facility coordinator Dr Vitaliy Gorbatyuk for his kind help on 2D HMBC measurements. JH is grateful for the support from National Science Foundation (CBET-1705566). The SEM/TEM studies were performed using the facilities in the UConn/FEI Center for Advanced Microscopy and Materials Analysis (CAMMA).

Notes and references

1 R. Shenhar, T. B. Norsten and V. M. Rotello, *Adv. Mater.*, 2005, **17**, 657–669.
2 J. Shan and H. Tenhu, *Chem. Commun.*, 2007, 4580–4598.
3 A. Sánchez-Iglesias, M. Grzelczak, T. Altantzis, B. Goris, J. Perez-Juste, S. Bals, G. Van Tendeloo, S. H. Donaldson Jr, B. F. Chmelka and J. N. Israelachvili, *ACS Nano*, 2012, **6**, 11059–11065.
4 J. Hu, T. Wu, G. Zhang and S. Liu, *J. Am. Chem. Soc.*, 2012, **134**, 7624–7627.
5 R. M. Choueiri, E. Galati, H. Thérien-Aubin, A. Klinkova, E. M. Larin, A. Querejeta-Fernández, L. Han, H. L. Xin, O. Gang and E. B. Zhulina, *Nature*, 2016, **538**, 79–83.
6 B. Liu, S. Thanneeru, A. Lopes, L. Jin, M. McCabe and J. He, *Small*, 2017, **13**, 1700091.
7 A. Sánchez-Iglesias, N. Claes, D. M. Solís, J. M. Taboada, S. Bals, L. M. Liz-Marzán and M. Grzelczak, *Angew. Chem.*, 2018, **130**, 3237–3240.
8 C. Yi, Y. Yang, B. Liu, J. He and Z. Nie, *Chem. Soc. Rev.*, 2020, DOI: 10.1039/C9CS00725C.
9 J. Song, P. Huang, H. Duan and X. Chen, *Acc. Chem. Res.*, 2015, **48**, 2506–2515.
10 Y. Liu, J. He, K. Yang, C. Yi, Y. Liu, L. Nie, N. M. Khashab, X. Chen and Z. Nie, *Angew. Chem.*, 2015, **127**, 16035–16038.
11 Z. Cao, D. Kim, D. Hong, Y. Yu, J. Xu, S. Lin, X. Wen, E. M. Nichols, K. Jeong, J. A. Reimer, P. Yang and C. J. Chang, *J. Am. Chem. Soc.*, 2016, **138**, 8120–8125.

12 Z. Cao, J. Derrick, J. Xu, R. Gao, E. Nichols, P. Smith, X. Liu, X. Wen, C. Coperet and C. Chang, *Angew. Chem., Int. Ed.*, 2018, **57**, 1–6.
13 J. He, X. Huang, Y.-C. Li, Y. Liu, T. Babu, M. A. Aronova, S. Wang, Z. Lu, X. Chen and Z. Nie, *J. Am. Chem. Soc.*, 2013, **135**, 7974–7984.
14 G. Chen, Y. Wang, M. Yang, J. Xu, S. J. Goh, M. Pan and H. Chen, *J. Am. Chem. Soc.*, 2010, **132**, 3644–3645.
15 A. B. Lowe, B. S. Sumerlin, M. S. Donovan and C. L. McCormick, *J. Am. Chem. Soc.*, 2002, **124**, 11562–11563.
16 M. K. Corbierre, N. S. Cameron and R. B. Lennox, *Langmuir*, 2004, **20**, 2867–2873.
17 E. R. Zubarev, J. Xu, A. Sayyad and J. D. Gibson, *J. Am. Chem. Soc.*, 2006, **128**, 15098–15099.
18 Z. Nie, D. Fava, E. Kumacheva, S. Zou, G. C. Walker and M. Rubinstein, *Nat. Mater.*, 2007, **6**, 609.
19 Z. Nie, D. Fava, M. Rubinstein and E. Kumacheva, *J. Am. Chem. Soc.*, 2008, **130**, 3683–3689.
20 B. Wang, B. Li, B. Zhao and C. Y. Li, *J. Am. Chem. Soc.*, 2008, **130**, 11594–11595.
21 J. He, Y. Liu, T. Babu, Z. Wei and Z. Nie, *J. Am. Chem. Soc.*, 2012, **134**, 11342–11345.
22 R. Liang, J. Xu, R. Deng, K. Wang, S. Liu, J. Li and J. Zhu, *ACS Macro Lett.*, 2014, **3**, 486–490.
23 T. K. Mandal, M. S. Fleming and D. R. Walt, *Nano Lett.*, 2002, **2**, 3–7.
24 J. Raula, J. Shan, M. Nuopponen, A. Niskanen, H. Jiang, E. I. Kauppinen and H. Tenhu, *Langmuir*, 2003, **19**, 3499–3504.
25 J. Song, L. Cheng, A. Liu, J. Yin, M. Kuang and H. Duan, *J. Am. Chem. Soc.*, 2011, **133**, 10760–10763.
26 M.-T. Lee, C.-C. Hsueh, M. S. Freund and G. S. Ferguson, *Langmuir*, 1998, **14**, 6419–6423.
27 G. E. Poirier, T. M. Herne, C. C. Miller and M. J. Tarlov, *J. Am. Chem. Soc.*, 1999, **121**, 9703–9711.
28 E. C. Hurst, K. Wilson, I. J. Fairlamb and V. Chechik, *New J. Chem.*, 2009, **33**, 1837–1840.
29 J. Vignolle and T. D. Tilley, *Chem. Commun.*, 2009, 7230–7232.
30 K. V. Ranganath, J. Kloesges, A. H. Schäfer and F. Glorius, *Angew. Chem., Int. Ed.*, 2010, **49**, 7786–7789.
31 P. Lara, O. Rivada-Wheelaghan, S. Conejero, R. Poteau, K. Philippot and B. Chaudret, *Angew. Chem.*, 2011, **123**, 12286–12290.
32 C. Richter, K. Schaepe, F. Glorius and B. J. Ravoo, *Chem. Commun.*, 2014, **50**, 3204–3207.
33 S. G. Song, C. Satheeshkumar, J. Park, J. Ahn, T. Premkumar, Y. Lee and C. Song, *Macromolecules*, 2014, **47**, 6566–6571.
34 M. J. MacLeod and J. A. Johnson, *J. Am. Chem. Soc.*, 2015, **137**, 7974–7977.
35 A. V. Zhukhovitskiy, M. J. MacLeod and J. A. Johnson, *Chem. Rev.*, 2015, **115**, 11503–11532.
36 M. D. de los Bernardos, S. Perez-Rodriguez, A. Gual, C. Claver and C. Godard, *Chem. Commun.*, 2017, **53**, 7894–7897.
37 S. Engel, E.-C. Fritz and B. J. Ravoo, *Chem. Soc. Rev.*, 2017, **46**, 2057–2075.
38 K. Klauke, I. Gruber, T.-O. Knedel, L. Schmolke, J. Barthel, H. Breitzke, G. Buntkowsky and C. Janiak, *Organometallics*, 2018, **37**, 298–308.
39 C. A. Smith, M. R. Narouz, P. A. Lummis, I. Singh, A. Nazemi, C.-H. Li and C. M. Crudden, *Chem. Rev.*, 2019, **119**, 4986–5056.
40 D. Bourissou, O. Guerret, F. P. Gabbaï and G. Bertrand, *Chem. Rev.*, 2000, **100**, 39–92.
41 T. Rovis and S. P. Nolan, *Synlett*, 2013, 1188–1189.
42 S. P. Nolan, *N-Heterocyclic Carbenes: Effective Tools for Organometallic Synthesis*, John Wiley & Sons, 2014.
43 C. M. Crudden, J. H. Horton, I. I. Ebralidze, O. V. Zenkina, A. B. McLean, B. Drevniok, Z. She, H.-B. Kraatz, N. J. Mosey and T. Seki, *Nat. Chem.*, 2014, **6**, 409.
44 A. Ferry, K. Schaepe, P. Tegeder, C. Richter, K. M. Chepiga, B. J. Ravoo and F. Glorius, *ACS Catal.*, 2015, **5**, 5414–5420.
45 J. B. Ernst, C. Schwermann, G.-i. Yokota, M. Tada, S. Muratsugu, N. L. Doltsinis and F. Glorius, *J. Am. Chem. Soc.*, 2017, **139**, 9144–9147.
46 H. Rothfuss, N. D. Knofel, P. W. Roesky and C. Barner-Kowollik, *J. Am. Chem. Soc.*, 2018, **140**, 5875–5881.
47 R. Ye, A. V. Zhukhovitskiy, R. V. Kazantsev, S. C. Fakra, B. B. Wickemeyer, F. D. Toste and G. A. Somorjai, *J. Am. Chem. Soc.*, 2018, **140**, 4144–4149.
48 R. W. Y. Man, C.-H. Li, M. W. A. MacLean, O. V. Zenkina, M. T. Zamora, L. N. Saunders, A. Rousina-Webb, M. Nambo and C. M. Crudden, *J. Am. Chem. Soc.*, 2018, **140**, 1576–1579.
49 A. Rühling, K. Schaepe, L. Rakers, B. Vonhören, P. Tegeder, B. J. Ravoo and F. Glorius, *Angew. Chem., Int. Ed.*, 2016, **55**, 5856–5860.
50 L. Zhang, Z. Wei, S. Thanneeru, M. Meng, M. Kruzyk, G. Ung, B. Liu and J. He, *Angew. Chem., Int. Ed.*, 2019, **58**, 15834–15840.
51 M. R. Narouz, K. M. Osten, P. J. Unsworth, R. W. Man, K. Salorinne, S. Takano, R. Tomihara, S. Kaappa, S. Malola and C.-T. Dinh, *Nat. Chem.*, 2019, **11**, 419.
52 O. Santoro, A. Collado, A. M. Z. Slawin, S. P. Nolan and C. S. J. Cazin, *Chem. Commun.*, 2013, **49**, 10483–10485.
53 M. R. Furst and C. S. Cazin, *Chem. Commun.*, 2010, **46**, 6924–6925.
54 Y. D. Bidal, O. Santoro, M. Melaimi, D. B. Cordes, A. M. Z. Slawin, G. Bertrand and C. S. J. Cazin, *Chem. – Eur. J.*, 2016, **22**, 9404–9409.
55 K. Salorinne, R. W. Y. Man, C. H. Li, M. Taki, M. Nambo and C. M. Crudden, *Angew. Chem., Int. Ed.*, 2017, **56**, 6198–6202.
56 R. E. Wasylishen and G. Tomlinson, *Biochem. J.*, 1975, **147**, 605–607.
57 K. Pachler, R. Pachter and P. Wessels, *Org. Magn. Reson.*, 1981, **17**, 278–284.
58 M. E. Garner, W. Niu, X. Chen, I. Ghiviriga, K. A. Abboud, W. Tan and A. S. Veige, *Dalton Trans.*, 2015, **44**, 1914–1923.
59 V. Lewe, M. Preuss, E. A. Woźnica, D. Spitzer, R. Otter and P. Besenius, *Chem. Commun.*, 2018, **54**, 9498–9501.
60 M. Rodríguez-Castillo, D. Laurencin, F. Tielens, A. van der Lee, S. Clément, Y. Guari and S. Richeter, *Dalton Trans.*, 2014, **43**, 5978–5982.
61 Z. Cao, D. Kim, D. Hong, Y. Yu, J. Xu, S. Lin, X. Wen, E. M. Nichols, K. Jeong and J. A. Reimer, *J. Am. Chem. Soc.*, 2016, **138**, 8120–8125.
62 M. Rodríguez-Castillo, G. Lugo-Preciado, D. Laurencin, F. Tielens, A. van der Lee, S. Clément, Y. Guari, J. M. López-de-Luzuriaga,

M. Monge and F. Remacle, *Chem. – Eur. J.*, 2016, **22**, 10446–10458.
63 M. R. L. Furst and C. S. J. Cazin, *Chem. Commun.*, 2010, **46**, 6924–6925.
64 E. A. Doud, M. S. Inkpen, G. Lovat, E. Montes, D. W. Paley, M. L. Steigerwald, H. c. Vázquez, L. Venkataraman and X. Roy, *J. Am. Chem. Soc.*, 2018, **140**, 8944–8949.
65 D. S. Weinberger, M. Melaimi, C. E. Moore, A. L. Rheingold, G. Frenking, P. Jerabek and G. Bertrand, *Angew. Chem., Int. Ed.*, 2013, **52**, 8964–8967.
66 L. Jin, D. S. Weinberger, M. Melaimi, C. E. Moore, A. L. Rheingold and G. Bertrand, *Angew. Chem., Int. Ed.*, 2014, **53**, 9059–9063.
67 S. Díez-González, E. C. Escudero-Adán, J. Benet-Buchholz, E. D. Stevens, A. M. Slawin and S. P. Nolan, *Dalton Trans.*, 2010, **39**, 7595–7606.
68 J. Crespo, Y. Guari, A. Ibarra, J. Larionova, T. Lasanta, D. Laurencin, J. M. López-de-Luzuriaga, M. Monge, M. E. Olmos and S. Richeter, *Dalton Trans.*, 2014, **43**, 15713–15718.